Organic & Biomolecular Chemistry

RSC Publishing

PAPER

View Article Online
View Journal | View Issue

Cite this: *Org. Biomol. Chem.*, 2013, **11**, 4077

Dibenzotetraaza[14]annulene–adenine conjugate recognizes complementary poly dT among ss-DNA/ss-RNA sequences†

Marijana Radić Stojković,[a] Marko Škugor,[a] Sanja Tomić,[a] Marina Grabar,[a] Vilko Smrečki,[a] Łukasz Dudek,[b] Jarosław Grolik,[b] Julita Eilmes*[b] and Ivo Piantanida*[a]

Received 14th March 2013,
Accepted 11th April 2013

DOI: 10.1039/c3ob40519b

www.rsc.org/obc

Among three novel DBTAA derivatives only the DBTAA–propyl–adenine conjugate **1** showed recognition of the consecutive oligo dT sequence by increased affinity and specific induced chirooptical response in comparison to other single stranded RNA and DNA; whereby of particular importance is the up until now unique efficient differentiation between dT and rU. At variance, its close analogue DBTAA–hexyl–adenine **2** did not reveal any selectivity between ss-DNA/RNA pointing out the important role of steric factors (linker length); moreover non-selectivity of the reference compound (**3**, lacking adenine) stressed the importance of adenine interactions in the **1** selectivity.

Introduction

Both, DNA and RNA exhibit a wide range of structural topologies, among which different single stranded (ss-) sequences are quite numerous. While ss-sequences are a ubiquitous part of the RNA folding landscape, there are fewer observations of stable ss-DNA cases, such as hairpins[1] or abasic sites,[2] to name but some of them. Since ds-DNA is protected from reaction with a number of chemical and biological nucleases,[3] many studies have been aimed at exploiting the vulnerable ss-DNA. A number of small molecules were synthesized that bind specifically at abasic lesions with the idea to inhibit the DNA repair system and in that way pronounce the action of anti-tumor drugs.[4] Moreover, recently many research groups have explored the potential of DNA as a template for arraying multi-chromophoric systems, among which non-covalent ss-DNA-associated dyes have attracted considerable attention.[5]

Until now research has shown that aryl–nucleobase conjugates efficiently recognized complementary nucleobases by affinity increase,[4] Zn–cyclene derivatives showed highly selective interactions with uracil and thymine caused by specific coordination of Zn with two keto groups.[6] Very recently, abasic sites and single base bulges in DNA were efficiently recognized by metalloinsertors,[7] and a small-ligand-immobilized biosensor was applied for detecting thymine-related single-nucleotide polymorphisms (SNPs).[8] However, longer oligo-dT sequences were not specifically recognised until now, especially in respect to closely related uracil analogues. Within the last decade we showed that small modifications in the structure of aryl–nucleobase conjugates can control their selectivity toward various ss- and ds- polynucleotide sequences.[9]

On the other hand, for the dibenzotetraaza[14]annulene (DBTAA) derivatives we recently showed that the interactions of side-chains can finely tune selectivity toward various DNA/RNA and consequently control their biological activity.[10a] Specific properties of the DBTAA moiety, such as larger aromatic surface than the most of until now used aryl-moieties and pronounced out-of-plane flexibility, offered intriguing possibilities in the design of novel aryl–nucleobase conjugates. The very last generation of DBTAA derivatives showed high (sub-micromolar) DNA/RNA affinity and selectivity toward dA–dT over dG–dC sequences,[10b] the latter property inspiring us to prepare DBTAA–adenine derivatives (Scheme 1), with the aim of the selective recognition of complementary nucleobases (rU and/or dT) within the DNA/RNA sequences. Previous results showed that structural features of the targeted recognition process sometimes strongly depend on the linker between the large aromatic moiety and nucleobase,[9b] therefore we varied the length of the linker between DBTAA and adenine (**1** and **2**), and as a reference compound we prepared the DBTAA lacking a nucleobase (**3**).

[a]*Division of Organic Chemistry and Biochemistry, Division of Physical Chemistry, NMR Centre, Ruđer Bošković Institute, Bijenička cesta 54, PO Box 180, HR-10002 Zagreb, Croatia. E-mail: pianta@irb.hr*

[b]*Department of Chemistry, Jagiellonian University, Ingardena 3, 30-060 Kraków, Poland*

†Electronic supplementary information (ESI) available: Characterization of **1–3**; detailed experiments with DNA and RNA, molecular modelling procedures and additional data. See DOI: 10.1039/c3ob40519b

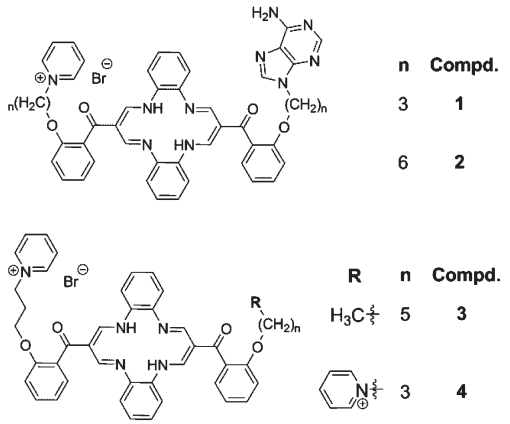

Scheme 1 Novel DBTAA–adenine conjugates **1** and **2**, reference compound **3**, and previously studied analogue **4**.[10b,c]

Results and discussion

Synthesis

DBTAA–adenine conjugates **1**, **2** and reference **3** were synthesized *via* two consecutive monoalkylations by a modified previously described method.[10c] The DBTAA–adenine conjugates **1** and **2** were synthesized in a two-step procedure involving reaction of the bis[2-(3-bromopropoxy)benzoyl]-5,14-dihydrodibenzo[*b*,*i*][1,4,8,11]tetraazacyclotetradecine (Scheme 2, **a**) with adenine in a 1 : 1 molar ratio, or monoalkylation of bis-(2-hydroxybenzoyl)-5,14-dihydrodibenzo[*b*,*i*][1,4,8,11]tetraaza-cyclotetradecine] (Scheme 2, **c**) using 9-(6-bromohexyl)adenine followed by incorporation of a pyridinium-alkoxy moiety according to the method reported earlier.[10c,11] A similar two-step procedure was employed for the preparation of unsymmetrically substituted product **3**.

Spectroscopic characterisation of buffered solutions of 1–3

Compounds **1–3** were moderately soluble in aqueous solutions (up to $c = 1 \times 10^{-3}$ mol dm^{-3}). Buffered aqueous solutions of the studied compounds were stable for several months. The absorbencies of **1–3** were proportional to their concentrations up to $c = 1 \times 10^{-4}$ mol dm^{-3}, changes of the UV/vis spectra on increasing the temperature up to 95 °C were negligible and reproducibility of UV/vis spectra upon cooling back to 25 °C was excellent. The UV/vis spectra of **1–3** were similar to previously studied analogue **4**,[10c] the differences in molar extinction coefficients† could be attributed to the additional adenine chromophore of **1**, **2** and lack of one pyridyl of **3**.

Study of interactions of 1–3 with ds-DNA in aqueous medium

The experiments with *calf thymus* (ct-)DNA (UV/vis titrations, thermal denaturation, viscometry, gel electrophoresis)† clearly excluded intercalation of DBTAA–adenine conjugates **1–3** into ds-DNA. Only **1** showed induced CD bands at $\lambda > 300$ nm upon binding to ct-DNA,† which can be attributed to the well-organized agglomeration within the minor groove. At variance to **1–3**, the previously studied DBTAA analogue **4**[10b] intercalated into ct-DNA, showing significantly stronger affinity and thermal stabilization effects. Such pronounced difference in the binding mode to ds-DNA could be attributed to distinct structural differences: the two positively charged pyridine moieties of **4** are both small enough to allow intercalation of DBTAA into DNA combined with simultaneous electrostatic interactions of the two positive charges with the negative DNA backbone. At variance to **4**, novel compounds **1**, **2** have only one positive charge (thus lowering the attracting forces) and in addition large and neutral adenine of **1**, **2** could by intramolecular stacking on DBTAA compete with intercalation of DBTAA within ds-DNA basepairs. More surprising was the non-intercalative binding mode of reference **3**, due to its close similarity to **4**. The differences between **3** and **4** in aqueous solution were significantly lower solubility of the former and tendency to form a colloidal system upon addition of ct-DNA even at μM concentrations. Particularly the latter observation suggested the preferred aggregation of **3** along hydrophobic ds-DNA grooves instead of intercalation. However, more detailed

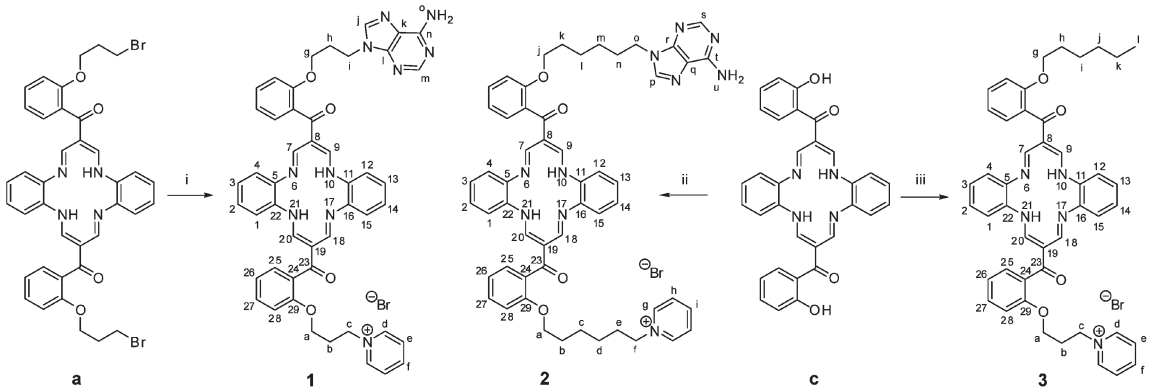

Scheme 2 Starting compounds **a**) and **c**) are prepared as described previously.[10c,11a] Preparation of the products **1–3**. i: (1) adenine, NaH, DMF, (2) pyridine; ii: (1) 9-(6-bromohexyl)adenine, potassium carbonate, DMF, (2) 1,6-dibromohexane, potassium carbonate, DMF, (3) pyridine; iii: (1) 1-bromohexane, potassium carbonate, DMF, (2) 1,3-dibromopropane, potassium carbonate, DMF, (3) pyridine.

studies of **1–3** with synthetic ds-DNA/RNA of homogenous basepair composition are necessary prior to any definite conclusion.

Study of interactions of 1–3 with ss-DNA and ss-RNA in aqueous medium

With the idea that the DBTAA moiety will easily intercalate within single stranded (ss-) DNA/RNA (much more flexible than ds-DNA), while the adenine of **1**, **2** could form H-bonds with complementary nucleobases, we studied the interaction of **1–3** with a series of homogeneous RNA and DNA polynucleotides.

The UV/vis titrations of **1–3** with ss-DNA and ss-RNA revealed pronounced hypochromic effects >300 nm (Table 1, ESI†), characteristic of aromatic stacking interactions of chromophore (DBTAA) with nucleobases. The affinities of **1–3** toward most of the ss-DNA/RNA were similar, the only exception being an intriguing two orders of magnitude higher affinity of **1** toward poly dT (Table 1, Fig. 1).

To get information about the changes induced by the small molecule on the spectroscopic properties of the polynucleotide, CD spectroscopy was applied as a highly sensitive method to evaluate conformational changes in the secondary structure of polynucleotides.[12] Additionally, the induced (I)CD spectrum which can appear upon binding of achiral small molecules to polynucleotides could give useful information about modes of interaction related to the orientation of a small molecule with respect to the DNA/RNA chiral axis.[12,13] It is of note that **1–3** are achiral and therefore do not possess intrinsic CD spectrum. Therefore, we performed CD experiments with **1–3**/polynucleotide complexes and indeed, addition of poly dT resulted in the specific induced (I)CD band of **1**, while with other ss-DNA/RNA **1** did not show any ICD band (Fig. 2 and ESI†). The plot of ICD band intensity against *c*(poly dT) for the **1**/poly dT complex agreed well with the UV/vis titration (Fig. 1),

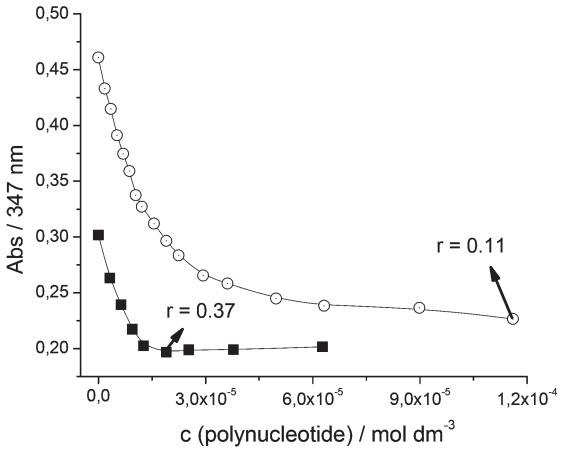

Fig. 1 Dependence of absorbance of **1** at λ_{max} = 347 nm on *c* (■, poly dT) and *c* (○, poly rU), at pH = 7, sodium cacodylate buffer, *I* = 0.05 mol dm^{-3}. Ratio *r*[**1**]/[polynucleotide] at the titration endpoint marked by an arrow.

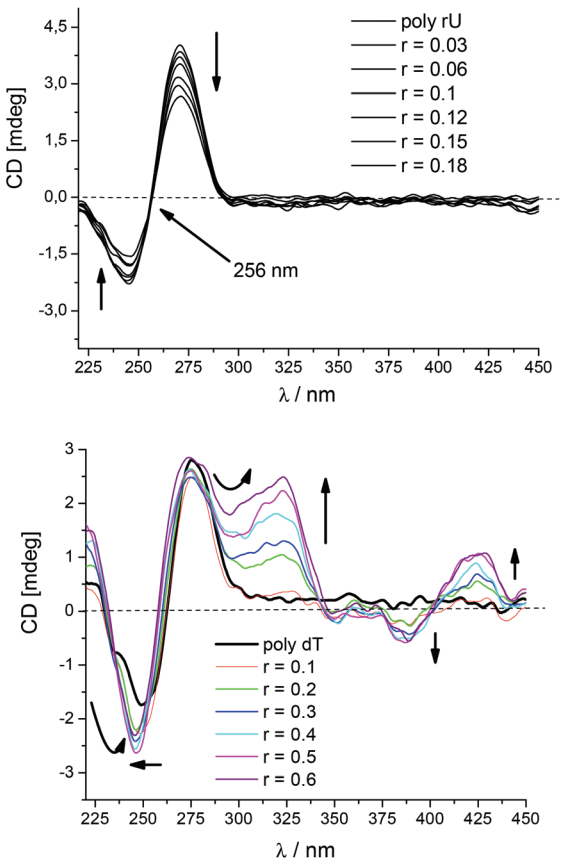

Fig. 2 Changes in CD spectra of poly rU (up) and poly dT (down); *c* (polynucleotide) = 3.0 × 10^{-5} mol dm^{-3} upon titration with **1**. Done at pH = 7, sodium cacodylate buffer, *I* = 0.05 mol dm^{-3}.

Table 1 Binding constants (log K_s)[ab] calculated from the UV/vis titrations of **1–3** with ss-polynucleotides at pH 7.0 (buffer sodium cacodylate, *I* = 0.05 mol dm^{-3})

	1		**2**		**3**	
	H^c/%	log K_s	H^c/%	log K_s	H^c/%	log K_s
Poly rC	46	6.2 ± 0.04	77	5.9 ± 0.03	—[d]	5–6[d]
Poly rA	78	5.4 ± 0.04	67	5.1 ± 0.02	—[d]	5–6[d]
Poly rG	25	6.5 ± 0.04	25[d]	5–6[d]	—[d]	5–6[d]
Poly rU	59	6.1 ± 0.05	62[d]	5–6[d]	—[d]	5–6[d]
Poly dT	30	8.7 ± 0.04	—[d]	—[d]	—[d]	5–6[d]
Poly dA	73	5.0 ± 0.03	—[d]	—[d]	—[d]	5–6[d]

[a] Processing of titration data by means of Scatchard equation[23] gave values of ratio $n_{[\text{bound 1–3}]/[\text{polynucleotide}]}$ = 0.2–0.7, for easier comparison all log K_s values were re-calculated for fixed n = 0.5. [b] Accuracy of n ± 10–30%, consequently log K_s values vary in the same order of magnitude. [c] $H_{346\ nm}$ = (Abs(**1–3**) − Abs(complex))/Abs(**1–3**)) × 100. [d] Formation of agglomerates close to equimolar concentration of compound and DNA/RNA hampered collection of a sufficient number of data, thus log K_s values could only be estimated.

supporting the high binding constant (Table 1). Such selectivity was not observed for reference compound **3**, or for the DBTAA–hexyl–adenine **2**, stressing the crucial importance of the adenine as well as the length of the linker connecting it to

DBTAA. Apparently, the shorter linker of **1** allows much more efficiently the intramolecularly-stacked DBTAA–adenine structure, necessary for the fine tuning of the adenine to thymine orientation.

The UV/vis and CD experiments performed with dT decamer also revealed high affinity and the same ICD bands.† However, the corresponding experiments of **1** with mononucleotides (AMP, GMP, CMP, UMP, TMP)† yielded at least an order of magnitude lower log K_s values in comparison with the corresponding ss-RNA/DNA (for thymine the difference between TMP and poly dT binding constant was 3 orders of magnitude). Moreover, the absence of any ICD band of **1** upon adding the aforementioned mononucleotides stressed the essential impact of several consecutive dT in the oligonucleotide sequence for achieving efficient helical organisation and consequent ICD recognition.

A competitive experiment performed by adding up to 10-fold excess of poly U (Fig. 3) or other ss-DNA/RNA to the **1**/poly dT complex did not result in a decrease of the characteristic ICD bands (300–450 nm range), thus additionally supporting the affinity preference shown in the binding constants (Table 1).

The ^{1}H NMR experiments on **1** performed with both poly dT and oligo dT_{10} revealed strong broadening and pronounced decrease of **1** proton signals upon complex formation (not shown), which can be attributed to the involvement of **1** in intensive aromatic stacking interactions, possibly combined with additional aggregation of several complexed systems (due to order of magnitude higher concentrations of **1** in NMR experiments (**1** in 0.05 mM and oligo dT 0.1 mM concentration) in comparison to previously described spectrophotometric methods). However, the resulting weak and very broad proton signals were unsuitable for efficient NOE experiments, hampering the determination of intramolecular contacts in **1**/oligo dT_{10}.

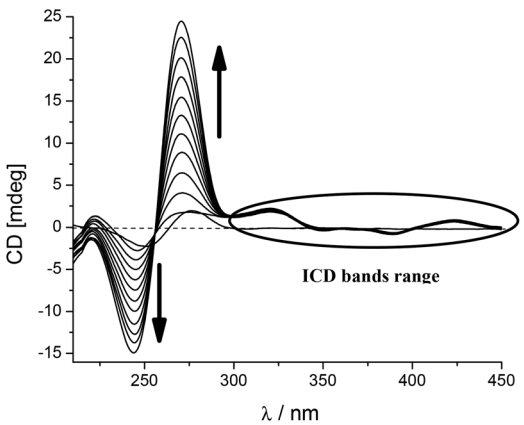

Fig. 3 Changes in the CD spectra of **1**/poly dT complex (c(poly dT) = 1.5 × 10^{-5} mol dm^{-3}; c(**1**) = 7.5 × 10^{-6} mol dm^{-3}), upon addition of a 1–10 fold excess of poly U (ratio = [poly U]/[poly dT]). Done at pH 7.0, buffer sodium cacodylate, I = 0.05 mol dm^{-3}. Increase of CD bands intensity at 245 nm and 275 nm corresponds to the CD spectrum of free poly rU.

Molecular modelling

The most intriguing result was the up until now unmatched property of **1** to bind significantly stronger to poly dT than to poly rU and give a specific chirooptical signal for poly dT. To shed more light on this recognition process, we addressed the **1**/dT and **1**/rU complexes by molecular modelling. Analysis started from the same geometry: the DBTAA moiety was inserted between adjacent nucleobases (supported by UV/vis and ICD results), adenine forming H-bonds with rU or dT (ESI, Fig. S17 and S18†). The complexes were solvated, energy optimized, and subjected to MD simulations. The complex between poly dT and **3** was built from the **1**–poly dT complex by removing adenine. The initial aromatic stacking between DBTAA and the nucleobases of the complexes was not disrupted during the 3 ns of MD simulations at room temperature.

Results pointed to the pronounced difference between the final structures of the **1**/dT and **1**/rU complexes. Namely, in the **1**/dT complex (Fig. 4) the intramolecular stacking between adenine and DBTAA is preserved (imidazole ring to DBTAA-double bond distance 3.36 Å) and adenine with one of the *o*-xylyl linkers is at a 3.6–4 Å distance (angle of about 45°), suggesting either edge-to-face or face-to-face aromatic stacking interactions. Also, adenine forms two H-bonds with thymine, the latter stacked above the benzene of DBTAA at 3.81 Å. The thymines at the top and the bottom of the structure are stacked with adjacent thymines by a distance of 3.34 Å and 3.62 Å, respectively. From a viewpoint along the phosphate backbone axis, the sequence T-T-DBTAA-T-T formed a helical structure. Moreover, the thymine methyl is positioned above the centre of the pyridyl of **1** (distance 2.8 Å), suggesting the existence of a CH–π interaction. Such a binding motif of **1** can

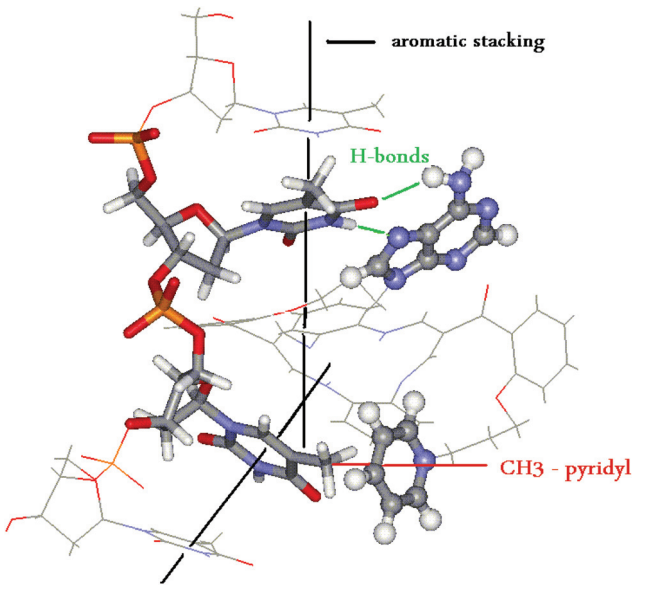

Fig. 4 Structure of the **1**/poly dT complex obtained by molecular modeling. Black lines mark the aromatic stacking interactions between thymines and DBTAA, green lines denote H-bonds between adenine and thymine, red lines mark the interaction between dT-methyl with the pyridyl of **1**.

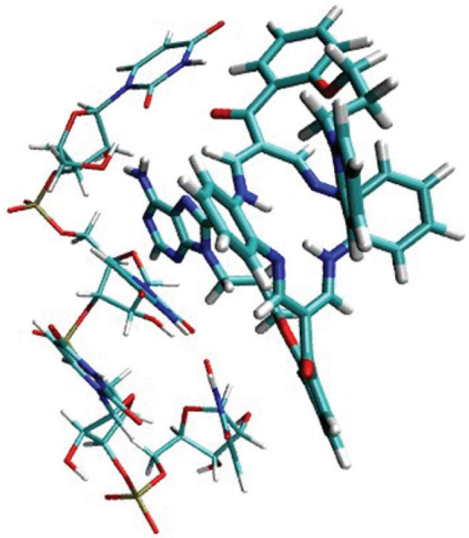

Fig. 5 Structure of the **1**/poly rU complex obtained by molecular modeling. Note the stacking of only one uracil with DBTAA and disruption of stacking between uracils along the poly rU helical axis.

be repeated along poly dT forcing the thymidines into an intensively stacked, helical structure, which is clearly better organized than the intrinsic structure of the free poly dT.[14] Therefore, the evident aromatic stacking of the DBTAA moiety between two thymines in the well-ordered structure of the **1**/poly dT complex (Fig. 4) controlled the uniform orientation of DBTAA chromophore transition moments with respect to the chiral axis of the newly formed helical structure, which in turn can explain the induced ICD bands above 300 nm, characteristic for the DBTAA moiety.[12,13]

The structure of the **1**/poly rU complex obtained by modelling from the same starting point as the previous dT-version (Fig. 5) is stabilized mostly by aromatic stacking interactions between various uracils with the DBTAA phenyl (3.37 Å), and *o*-xylyl linkers (3.87 Å and 3.81 Å). Furthermore, the adenine is edge-to-face oriented pointing proton H8 to the centre of DBTAA (3.7 Å). Hydrogen bonds between adenine (of **1**) and uracil are missing and uracil does not have a methyl to form an interaction with the pyridyl of **1**, instead, the pyridyl is stacked with the phenyl-DBTAA (3.7 Å). The structural outcome is oligo rU severely kinked around a molecule of **1**, whereby the stacking between uracils is completely lost. Such a binding mode of **1** disrupts even more intrinsically the poorly organised poly rU structure, which decreases the intensity of the already weak CD bands of poly rU. Consequently, the absence of significant chiral helicity of polynucleotide/**1** complex completely failed to induce any ICD band above 300 nm.

Application of an identical modelling approach to reference compound **3** yielded a completely different structure of the **3**/poly dT complex.† Compound **3** does not have adenine to form H-bonds with thymine and also the interaction between dT-methyl and **3**–pyridyl was missing. Such a poorly organized complex is not likely to give uniform organization of DBTAA units and thus no ICD bands were observed.

Conclusions

The here presented DBTAA–propyl–adenine conjugate **1** is to the best of our knowledge the first small molecule able to selectively recognize the ss-dT sequence in respect to the other homogenous ss-DNA/RNA (including rU) by both strongly increased affinity and specific spectroscopic (ICD) signal. Such selectivity of **1** is exceptionally intriguing because, both, rU and dT can form the same set of hydrogen bonds with adenine (this factor probably excluded poly rC), and both ss-polynucleotides are characterized by similar, poorly organized secondary structure,[14] thus differing only by C5-methyl group specific for thymine and one additional sugar 2′-OH group of rU, respectively. Intriguingly, in analogous double stranded polynucleotide systems the thymine-methyl also has an important role in double stranded helix stabilisation. For instance, poly(dA)–poly(dT) has 50% greater stability than poly(dA)–poly(dU) as a result of the dT-methyl impact.[15] Furthermore, a study of the significant differences in stability of DNA *vs.* RNA double stranded helices revealed that the contribution of dTC-5 methyl groups is always stabilizing, while 2′-OH groups (present only in RNA) can be stabilizing but also destabilizing, depending on the type of complex.[16] Thus, taking into account an estimation of C5-methyl group contribution to ds-DNA stabilisation of about 0.3 kcal mol^{-1} per AT pair,[17] combined with the absence of the 2′-OH group in poly dT (which increases the adjustability of the polynucleotide), can explain the more efficient adjustment of **1** upon binding to poly dT in comparison to poly rU. This is in accordance with the here presented molecular modelling results, showing that the main factors regulating **1**–poly dT selectivity are (a) self-stacked DBTAA–adenine system, which is favoured only by the short linker of **1** but completely lost for the longer linker of **2**, (b) H-bonding between adenine and thymine (not present in **1**/poly rU complex and reference compound **3**); (c) interaction between thymine-methyl and pyridyl of **1** (not present in the model of **1**/poly rU).

The presented results will have high practical importance in the supramolecular design of novel small molecules targeting dT-based sequences, either for ss-DNA or ds-DNA based supramolecular constructs[5] or in biological applications; for instance marking of the oligo (dT)-cellulose commonly used for tRNA purification,[18] or T–T sequences which are aside from guanine-sequences the most sensitive to radical-induced damage.[19] Furthermore, compounds **1–4** are azamacrocyclic ligands and thus have additional potential to bind metal cations,[20] such metal complexes offering a variety of different interactions with DNA/RNA. Preliminary experiments with **4** and several metal cations of biological interest (*e.g.* Zn^{2+}, Cu^{2+}, La^{3+}) revealed surprisingly low stability of complexes under biologically relevant conditions ($K_s < 10^{-4}$ M^{-1}). Ongoing experiments try to address that issue by the design of novel

compounds with biologically relevant stability of metal complexes.

Experimental

Synthetic procedures

(7-{2-[3-(Aden-9-yl)propoxy]benzoyl}-16-{2-[3-(*N*-pyridinium-1-yl)propoxy]benzoyl}-5,14-dihydrodibenzo[*b*,*i*][1,4,8,11]tetraazacyclotetradecine bromide) (1). A mixture consisting of adenine (0.266 g, 1.973 mmol), 60% NaH (0.059 g, 1.408 mmol) in anhydrous DMF (5 mL) was stirred for 1 h at room temperature. Compound **a** (0.76 g, 0.986 mmol) dissolved in anhydrous DMF (60 mL) was added and the reaction mixture was stirred at 40 °C for 5 min, then for 3 h at room temperature. The reaction mixture was then transferred to a separatory funnel and partitioned between dichloromethane (150 mL) and water (100 mL). The organic layer was separated, washed with water (2 × 100 mL), dried over anhydrous magnesium sulfate, concentrated to a small volume and chromatographed on a column of silica gel using dichloromethane–methanol (40 : 2 v/v) as eluent. The main orange fraction was collected and evaporated to dryness. A residue was dissolved in pyridine (6 mL) and stirred for 9 h at 45 °C. the excess of pyridine was removed under diminished pressure and the residue was chromatographed on a column with basic aluminium oxide, using dichloromethane–methanol (20 : 3 v/v) as eluent. The main orange fraction was collected, concentrated to a small volume and diluted with *n*-hexane to precipitate an orange product (0.144 g, 16%).

Mp: 164–166 °C. ^{1}H-NMR (300 MHz, DMSO-d$_6$, δ): 2.10 (2H, m, H^h), 2.28 (2H, m, H^b), 4.03 (2H, t, J = 6.0 Hz, H^g), 4.12 (4H, m, H^a, H^i), 4.65 (2H, t, J = 6.9 Hz, H^c), 7.04 (2H, s, H^o), 7.08–7.24 (12H, m, H^1–H^4, H^{12}–H^{15}, H^{26}, H$^{26'}$, H^{28}, H$^{28'}$), 7.35 (2H, m, H^{25}, H$^{25'}$), 7.50 (2H, m, H^{27}, H$^{27'}$), 7.85 (1H, s, H^m), 7.90 (1H, s, H^j), 7.96 (2H, m, H^e), 8.36 (2H, d, J = 6.5 Hz, {H^7, H^9}/{H^{18}, H^{20}}), 8.45–8.52 (3H, m, {H^7, H^9}/{H^{18}, H^{20}}, H^f), 8.98 (2H, m, H^d), 14.20 (2H, m, H^{10}, H^{21}). ^{13}C-NMR (75 MHz, DMSO-d$_6$, δ): 29.0 (C^h), 30.0 (C^b), 58.3 (C^c), 65.0 (C^a), 65.2 (C^g), 109.8, 110.2 (C^8, C^{19}), 112.7, 113.0 (C^{28}, C$^{28'}$), 115.3, 115.4 (C^1, C^4, C^{12}, C^{15}), 118.7 (C^k), 121.0, 121.1 (C^{26}, C$^{26'}$), 126.7 (C^2, C^3, C^{13}, C^{14}), 127.8 (C^e), 128.6, 128.8 (C^{24}, C$^{24'}$), 129.2 (C^{25}, C$^{25'}$), 131.4, 131.5 (C^{27}, C$^{27'}$), 136.2, 136.3 (C^5, C^{11}, C^{16}, C^{22}), 140.4 (C^j), 144.6 (C^d), 145.4 (C^f), 149.3 (C^l), 152.1 (C^m), 152.4, 152.6 (C^7, C^9, C^{18}, C^{20}), 154.8, 155.1 (C^{29}, C$^{29'}$), 155.7 (C^n), 191.2, 191.4 (C^{23}, C$^{23'}$). IR (ATR) ν_{max} (cm^{-1}): 1254, 1285, 1326, 1414, 1445, 1487, 1557, 1591, 1642, 2876, 2959, 3059, 3203, 3355. MS (ESI) *m*/*z* found: 823.6. Calc. for $C_{48}H_{43}N_{10}O_4^+$: 823.35. Anal. found: C, 61.47; H, 4.98; N, 14.71. Calc. for $C_{48}H_{43}N_{10}O_4Br{\cdot}2H_2O$: C, 61.34; H, 5.04; N, 14.90%.

(7-{2-[6-(Aden-9-yl)hexoxy]benzoyl}-16-{2-[6-(*N*-pyridinium-1-yl)hexoxy]benzoyl}-5,14-dihydrodibenzo[*b*,*i*][1,4,8,11]tetraazacyclotetradecine bromide) (2). A reaction mixture consisting of compound **c** (0.2 g, 0.378 mmol), anhydrous potassium carbonate (0. 104 g, 0.757 mmol) and 9-(6-bromohexyl)adenine (0.056 g, 0.189 mmol) in anhydrous DMF (40 mL) was stirred for 10 h at 65 °C. 1,6-Dibromohexane (0.7 mL, 4.54 mmol) and anhydrous potassium carbonate (0.026 g, 0.189 mmol) were then added and stirring was continued for 24 h at room temperature. The reaction mixture was transferred to a separatory funnel and partitioned between dichloromethane (20 mL) and water (100 mL). A small amount of solid KBr was added to improve separation of the phases. The organic layer was separated and washed thoroughly with water (5 × 30 mL), dried over anhydrous magnesium sulfate, concentrated to a small volume and chromatographed on a column of silica gel using dichloromethane–methanol, (20 : 0.4 v/v) as eluent. The second fraction was collected from the two orange ones of highest intensity. It was evaporated to dryness, dissolved in a small volume of chloroform and once more chromatographed on a column of silica gel, using chloroform–methanol (20 : 0.4 v/v) as eluent. The main fraction was collected, evaporated to dryness and a solid residue was dissolved in pyridine (5 mL). The mixture was stirred for 7 h at 45 °C, then pyridine was removed under diminished pressure and the solid residue was chromatographed on a column with basic aluminium oxide, using dichloromethane–methanol (20 : 2 v/v) as eluent. The main orange fraction was collected and evaporated to dryness. An orange microcrystalline product was obtained by slow evaporation of methylene chloride solution of the crude material (0.042 g, 11%).

Mp: 194–196 °C. ^{1}H-NMR (300 MHz, DMSO-d$_6$, δ): 0.97–1.28 (8H, m, aliphatic chain), 1.50 (6H, m, aliphatic chain), 1.64 (2H, m, aliphatic chain), 3.86 (2H, t, J = 7 Hz, H^j), 3.95 (4H, m, H^a, H^o), 4.40 (2H, t, J = 7.5 Hz, H^f), 7.03–7.19 (14H, m, H^1–H^4, H^{12}–H^{15}, H^{26}, H$^{26'}$, H^{28}, H$^{28'}$, H^u), 7.34 (2H, m, H^{25}, H$^{25'}$), 7.49 (2H, m, H^{27}, H$^{27'}$), 7.85 (1H, s, H^s), 7.97 (1H, s, H^p), 8.05 (2H, m, H^h), 8.44 (4H, m, H^7, H^9, H^{18}, H^{20}), 8.53 (1H, m, H^i), 8.93 (2H, m, H^g), 14.20 (2H, m, H^{10}, H^{21}). ^{13}C-NMR (75 MHz, DMSO-d$_6$, δ): 24.8, 24.9, 25.0, 25.6, 28.2, 28.4, 29.1, 30.6 (C^b–C^e, C^k–C^n), 42.5 (C^o), 60.5 (C^f), 67.7, 67.8 (C^a, C^j), 110.1 (C^8, C^{19}), 112.5 (C^{28}, C$^{28'}$), 115.2 (C^1, C^4, C^{12}, C^{15}), 118.7 (C^q), 120.8 (C^{26}, C$^{26'}$), 126.7 (C^2, C^3, C^{13}, C^{14}), 128.0 (C^h), 128.7, 128.7 (C^{24}, C$^{24'}$), 129.4, 129.3 (C^{25}, C$^{25'}$), 131.5, 131.7 (C^{27}, C$^{27'}$), 136.1, 136.1 (C^5, C^{11}, C^{16}, C^{22}), 140.4 (C^p), 144.4 (C^g), 145.4 (C^i), 149.3 (C^r), 152.2 (C^s), 152.5 (C^7, C^9, C^{18}, C^{20}), 155.2, 155.3 (C^{29}, C$^{29'}$), 155.8 (C^t), 191.6 (C^{23}, C$^{23'}$). IR (ATR) ν_{max} (cm^{-1}): 1239, 1290, 1308, 1414, 1447, 1485, 1558, 1585, 1652, 1679, 2875, 2931, 3059, 3116, 3242, 3374. MS (ESI) *m*/*z* found 908.3. Calc. for $C_{54}H_{55}N_{10}O_4^+$: 907.44. Anal. found: C, 65.62; H, 5.95; N, 14.05. Calc. for $C_{54}H_{55}N_{10}O_4Br$: C, 65.65; H, 5.61; N, 14.18%.

(7-(2-Hexoxybenzoyl)-16-{2-[3-(*N*-pyridinium-1-yl)propoxy]-benzoyl}-5,14-dihydrodibenzo[*b*,*i*][1,4,8,11]tetraazacyclotetradecine bromide) (3). A reaction mixture consisting of compound **c** (1 g, 1.892 mmol), 1-bromohexane (0.319 mL, 2.27 mmol) and anhydrous potassium carbonate (0.313 g, 2.27 mmol) in anhydrous DMF (130 mL) was stirred at 60 °C, for 3 h. The mixture was cooled down, transferred to a separatory funnel and partitioned between chloroform(150 mL) and water (200 mL). A few drops of hydrobromic acid solution were added to improve separation of the phases. The organic layer was separated and washed thoroughly with water (7 × 100 mL),

dried over anhydrous magnesium sulfate and evaporated to dryness. The solid residue was dried at 55 °C *in vacuo* and added to a reaction mixture consisting of 1,3-dibromopropane (1.92 mL, 18.92 mmol) and anhydrous potassium carbonate (0.523 g, 3.784 mmol) in anhydrous DMF (30 mL). The mixture was stirred at room temperature for 24 h, then transferred to separatory funnel and partitioned between toluene (100 mL) and water (250 mL). A small amount of solid KBr was added to improve separation of the phases. The organic layer was separated, washed with water (7 × 100 mL) and dried over anhydrous magnesium sulfate. The solvent was evaporated; the residue was dissolved in a small amount of methanol and left in a refrigerator for 12 h. The solid orange material was filtered off, washed with methanol and dried. It was then chromatographed twice on a column of silica gel using toluene–acetone (40 : 1 v/v) as eluent. A second orange fraction was collected, evaporated to dryness, dried *in vacuo* and dissolved in pyridine (4 mL). The mixture was stirred for 3 h at 60 °C. An excess of pyridine was evaporated and a solid residue was chromatographed on a column of silica gel using dichloromethane–methanol (10 : 1 v/v) as eluent. The solvents were evaporated and the residue was dried *in vacuo* to give an orange–red product (0.065 g, 4%).

Mp: 126–129 °C. ^{1}H-NMR (600 MHz, DMSO-d$_6$, δ): 0.56 (3H, t, J = 7.1 Hz, H^l), 0.98 (4H, m, H^j, H^k), 1.16 (2H, m, H^i), 1.48 (2H, m, H^h), 2.29 (2H, m, H^b), 3.96 (2H, t, J = 6.0 Hz, H^g), 4.12 (2H, t, J = 6.0 Hz, H^a), 4.65 (2H, t, J = 7 Hz, H^c), 7.07–7.19 (8H, m, H^2, H^3, H^{13}, H^{14}, H^{26}, H$^{26'}$, H^{28}, H$^{28'}$), 7.22–7.26 (4H, m, H^1, H^4, H^{12}, H^{15}), 7.34 (2H, m, H^{25}, H$^{25'}$), 7.50 (2H, m, H^{27}, H$^{27'}$), 8.00 (2H, m, H^e), 8.44 (4H, m, H^7, H^9, H^{18}, H^{20}), 8.53 (1H, m, H^f), 9.00 (2H, m, H^d), 14.22 (1H, t, J = 6.5 Hz, H^{10}/H^{21}), 14.27 (1H, t, J = 6.5 Hz, H^{10}/H^{21}). ^{13}C-NMR (75 MHz, DMSO-d$_6$, δ): 13.5 (C^l), 21.8, 25.1, 28.5, 30.1, 30.8 (C^b, C^h–C^k), 58.2 (C^c), 65.0, 67.8 (C^a, C^g), 110.0, 110.1 (C^8, C^{19}), 112.4, 113.1 (C^{28}, C$^{28'}$), 115.2, 115.4 (C^1, C^4, C^{12}, C^{15}), 120.8, 121.1 (C^{26}, C$^{26'}$), 126.7, 126.8 (C^2, C^3, C^{13}, C^{14}), 127.9 (C^e), 128.7, 128.7 (C^{24}, C$^{24'}$), 129.0, 129.3 (C^{25}, C$^{25'}$), 131.5, 131.6 (C^{27}, C$^{27'}$), 136.2 (C^5, C^{11}, C^{16}, C^{22}), 144.7 (C^d), 145.5 (C^f), 152.3, 152.5 (C^7, C^9, C^{18}, C^{20}), 154.8, 155.2 (C^{29}, C$^{29'}$), 191.3, 191.5 (C^{23}, C$^{23'}$). IR (ATR) ν_{max} (cm^{-1}): 1252, 1286, 1310, 1396, 1418, 1447, 1488, 1559, 1588, 1647, 2859, 2929, 3057, 3394. MS (ESI) m/z found: 732.6. Calc. for $C_{46}H_{46}N_5O_4^+$: 732.35. Anal. found: C, 66.07; H, 5.73; N, 8.25. Calc. for $C_{46}H_{46}N_5O_4Br{\cdot}1.3H_2O$: C, 66.07; H, 5.86; N, 8.37%.

Materials and methods

Elemental analyses were performed on an Elementar vario MICRO cube analyser. 1H and 13C NMR were run on a Bruker AVANCE II 300 and Bruker AVANCE III 600 spectrometers. Chemical shifts (δ) are expressed in parts per million and J values in hertz. Assignments of the NMR signals (for numeration of C-atoms and H-atoms see Scheme 2) were based on H–H COSY, HMBC and HSQC experiments, and literature data.[21] The H-2 and H-8 signals of adenine were differentiated using a known method involving deuteration experiments.[11b] ESI mass spectra were taken on a Bruker Esquire 3000 spectrometer. The IR spectra were recorded with a Thermo Fisher Scientific Nicolet IR200. Melting points were measured with the use of a Boethius apparatus and were uncorrected.

The UV/vis spectra were recorded on a Varian Cary 100 Bio spectrophotometer and CD spectra on JASCO J815 spectrophotometer at 25 °C using appropriate 1 cm path quartz cuvettes. For study of interactions with DNA and RNA, aqueous solutions of compounds buffered to pH 7.0 (buffer sodium cacodylate, I = 0.05 mol dm^{-3}) were used.

Polynucleotides were purchased as noted: poly dA, poly rA, poly rG, poly rC, poly rU, poly dT, oligo dT$_{10}$ (Sigma), calf thymus (ct)-DNA (Aldrich). Polynucleotides were dissolved in Na-cacodylate buffer, I = 0.05 mol dm^{-3}, pH 7.0. The calf thymus ctDNA was additionally sonicated and filtered through a 0.45 mm filter.[22] The polynucleotide concentration was determined spectroscopically as the concentration of phosphates. Spectrophotometric titrations were performed at pH 7.0 (I = 0.05 mol dm^{-3}, buffer sodium cacodylate) by adding portions of polynucleotide solution into the solution of the studied compound for UV/vis and for CD experiments were done by adding portions of compound stock solution into the solution of polynucleotide. Titration data were processed by the Scatchard equation.[23] Values for K_s and n given in Table 1 all have satisfactory correlation coefficients (>0.999). Thermal melting curves for DNA, RNA and their complexes with studied compounds were determined as previously described[24,25] by following the absorption change at 260 nm as a function of temperature. Absorbance of the ligands was subtracted from every curve and the absorbance scale was normalized. T_m values are the midpoints of the transition curves determined from the maximum of the first derivative and checked graphically by the tangent method.[24] The ΔT_m values were calculated subtracting T_m of the free nucleic acid from T_m of the complex. Every ΔT_m value here reported was the average of at least two measurements. The error in ΔT_m is ±0.5 °C.

Viscometry measurements were conducted with an Ubbelohde viscometer system AVS 370 (Schott). The temperature was maintained at 25 ± 0.1 °C. Aliquots of drug stock solutions were added to 3.0 ml of 5 × 10^{-4} mol dm^{-3} ct-DNA solution in sodium cacodylate buffer, I = 0.05 mol dm^{-3}, pH 7.0, with a compound to DNA phosphate ratio r less than 0.2. Dilution never exceeded 4% and was corrected for in the calculations. The flow times were measured at least five times optically with a deviation of ±0.2 s. The viscosity index α was obtained from the flow times at varying r according to the following eqn (1):[26]

$$L/L_0 = [(t_r - t_0)/(t_{\text{polynucleotide}} - t_0)]^{1/3} = 1 + \alpha \times r \qquad (1)$$

where t_0, $t_{\text{polynucleotide}}$ and t_r denote the flow times of buffer, free polynucleotide and polynucleotide complex at ratio $r_{[\text{compound}]/[\text{polynucleotide}]}$, respectively; L/L_0 is the relative DNA/RNA lengthening. The L/L_0 to $r_{[\text{compound}]/[\text{polynucleotide}]}$-plot was fitted to a straight line that gave slope α. The error in α is <0.1.

Agarose gel electrophoresis was performed on a 1% agarose in TAE buffer (pH8), using TAE as a running buffer,[27] applying

a constant voltage of 30 V for two hours, followed by quick staining of the gel with EB solution (0.5 μg mL^{-1}). Supercoiled plasmid DNA (pCI) was treated by compounds **1–3** and ethidium bromide as a reference for the intercalation.

Molecular modeling methods. Single stranded tetranucleotides, DNA (poly dT) and RNA (poly rU) were built with the program *nucgen*, a part of the Amber program suit.[28] Compounds **1** and **3** were built using module 'Builder' within program *InsightII*.[29] Complexes with ss-polynucleotides were built by intercalating the aromatic ring of DBTAA into the space between two adjacent bases in the middle of the polynucleotides. The adenine of **1** was oriented in such a way as to form two H-bonds with the polynucleotide-base, (thymine and uracil in the complex with ss-DNA and ss-RNA, respectively).

Parameterization was performed within the AMBER ff99SB force field of Duan *et al*.[30] and the general AMBER force field GAFF. Each complex was placed into the centre of the octahedral box filled with TIP3 type water molecules, a water buffer of 7 Å was used, and Na^+ ions were added to neutralize the systems. The solvated complexes were geometry optimized using steepest descent and conjugate gradient methods, 2500 steps of each. The optimized complexes were heated in steps of 100 K, each lasting 200 ps, while the volume was kept constant. The equilibrated systems were subjected to 3 ns of the productive unconstrained molecular dynamics (MD) simulation at constant temperature and pressure (300 K, 1 atm) using Periodic Boundary Conditions (PBC). The time step during the simulation was 1 fs and the temperature was kept constant using Langevin dynamics with a collision frequency of 1 ps^{-1}. The electrostatic interactions were calculated by the Particle Mesh Ewald (PME) method with cutoff-distance of 11 Å for the pairwise interactions in the real space. Geometry optimization and molecular dynamics (MD) simulations were accomplished using the AMBER 9 program package.

Acknowledgements

Financial support by the Ministry of Science, Education, Sport of Croatia (098-0982914-2918, 098-1191344-2860), the Grant (WCh-BW) Jagiellonian University, Krakow, Poland, European Regional Development Fund, Polish Innovation Economy Operational Program (contract POIG.02.01.00-12-023/08) is acknowledged.

Notes and references

1 S. Yoshizawa, G. Kawai, K. A. Watanabe, K. I. Miura and I. Hirao, *Biochemistry*, 1997, **36**, 4761.
2 H. Naegeli, in *Mechanism of DNA Damage Recognition in Mammalian Cells*, Springer-Verlag, Heidelberg, Germany, 1997.
3 C. Bailly and M. J. Waring, in *Methods in Molecular Biology*, Humana Press, Totowa, NJ, 1997, vol. 90, pp. 51–79.
4 (*a*) J. Lhomme, J. F. Constant and M. Demeunynck, *Biopolymers*, 1999, **52**, 65–83; (*b*) A. Martelli, J. F. Constant, M. Demeunynck, J. Lhomme and P. Dumy, *Tetrahedron*, 2002, **58**, 4291.
5 Y. N. Teo and E. T. Kool, *Chem. Rev.*, 2012, **112**, 4221.
6 E. Kimura and S. Aoki, *J. Am. Chem. Soc.*, 2000, **122**, 4542.
7 B. M. Zeglis, J. A. Boland and J. K. Barton, *J. Am. Chem. Soc.*, 2008, **130**, 7530.
8 S. Miura, S. Nishizawa, A. Suzuki, Y. Fujimoto, K. Ono, Q. Gao and N. Teramae, *Chem.–Eur. J.*, 2012, **17**, 14104.
9 (*a*) L.-M. Tumir, I. Piantanida, I. Juranović, Z. Meić, S. Tomić and M. Žinić, *Chem. Commun.*, 2005, 2561; (*b*) I. Juranović, Z. Meić, I. Piantanida, L.-M. Tumir and M. Žinić, *Chem. Commun.*, 2002, 1432; (*c*) V. Malinovski, L. Tumir, I. Piantanida, M. Žinić and H.-J. Schneider, *Eur. J. Org. Chem.*, 2002, 3785.
10 (*a*) M. Radić Stojković, I. Piantanida, M. Kralj, M. Marjanović, M. Žinić, D. Pawlica and J. Eilmes, *Bioorg. Med. Chem.*, 2007, **15**, 1795; (*b*) M. Radić Stojković, M. Marjanović, D. Pawlica, L. Dudek, J. Eilmes, M. Kralj and I. Piantanida, *New J. Chem.*, 2010, **34**, 500; (*c*) D. Pawlica, M. Radić Stojković, Ł. Dudek, I. Piantanida, L. Sieroń and J. Eilmes, *Tetrahedron*, 2009, **65**, 3980.
11 (*a*) I. Sigg, G. Haas and T. Winkler, *Helv. Chim. Acta*, 1982, **65**, 275; (*b*) T. Itahara, *J. Chem. Soc., Perkin Trans. 2*, 1996, 2695.
12 M. Eriksson and B. Norden, *Methods Enzymol.*, 2001, **340**, 68.
13 N. C. Garbett, P. A. Ragazzon and J. B. Chaires, *Nat. Protoc.*, 2007, **2**, 3166.
14 C. R. Cantor and P. R. Schimmel, in *Biophysical Chemistry*, WH Freeman and Co., San Francisco, vol. 3, 1980, pp. 1109–1181.
15 P. D. Ross and F. B. Howard, *Biopolymers*, 2003, **68**, 210.
16 S. H. Wang and E. T. Kool, *Biochemistry*, 1995, **34**, 4125.
17 T. B. Xia, J. SantaLucia, M. E. Burkard, R. Kierzek, S. J. Schroeder, X. Q. Jiao, C. Cox and D. H. Turner, *Biochemistry*, 1998, **37**, 14719.
18 J. Sambrook, E. F. Fritsch and T. Maniatis, in *Molecular Cloning, a Laboratory Manual*, vol. 1–3, Cold Spring Harbor Laboratory Press, New York, 1989.
19 G. B. Schuster, A. Ghosh, A. Joy, T. Douki and J. Cadet, *Org. Biomol. Chem.*, 2008, **6**, 916.
20 K. Lewinski and J. Eilmes, *J. Inclusion Phenom. Macrocyclic Chem.*, 2005, **52**, 261.
21 R. S. Iyer, M. W. Voehler and T. M. Harris, *J. Am. Chem. Soc.*, 1994, **116**, 8863.
22 J. B. Chaires, N. Dattagupta and D. M. Crothers, *Biochemistry*, 1982, **21**, 3933.
23 G. Scatchard, *Ann. N. Y. Acad. Sci.*, 1949, **51**, 660; J. D. McGhee and P. H. von Hippel, *J. Mol. Biol.*, 1976, **103**, 679.
24 I. Piantanida, B. S. Palm, P. Čudić, M. Žinić and H.-J. Schneider, *Tetrahedron*, 2004, **60**, 6225.
25 J. L. Mergny and L. Lacroix, *Oligonucleotides*, 2003, **13**, 515.

26 G. Cohen and H. Eisenberg, *Biopolymers*, 1969, **8**, 45; M. Wirth, O. Buchardt, T. Koch, P. E. Nielsen and B. Nordén, *J. Am. Chem. Soc.*, 1988, **110**, 932.
27 I. Lubitz, D. Zikich and A. Kotlyar, *Biochemistry*, 2010, **49**, 3567.
28 http://amber.scripps.edu/
29 INSIGHTII – Accelerys San Diego 2001–2008, http://accelrys.com/services/training/life-science/insight-migration.html
30 Y. Duan, C. Wu, S. Chowdhury, M. C. Lee, G. Xiong, W. Zhang, R. Yang, P. Cipelak, R. Luo and T. Lee, *J. Comput. Chem.*, 2003, **24**, 1999.